ELSEVIER

Polymer 43 (2002) 767–773

polymer

www.elsevier.com/locate/polymer

Mechanical properties of ethylene/1-hexene copolymers with tailored short chain branching distributions

C. Li Pi Shan, J.B.P. Soares*, A. Penlidis

Department of Chemical Engineering, Institute for Polymer Research, University of Waterloo, Waterloo, Ont., Canada N2L 3G1

Received 25 July 2001; received in revised form 27 September 2001; accepted 28 September 2001

Abstract

Recently, we have investigated a metallocene catalyst system that can produce polyethylene and ethylene/α-olefin copolymers with tailored molecular weight and short chain branching distributions (SCBD). Ethylene/α-olefin copolymers produced with this system have narrow molecular weight distributions as expected from metallocene catalysts. However, these copolymers are quite unique in that their SCBDs are broad and sometimes bimodal, similar to Ziegler–Natta LLDPE.

To examine the effect of these broad SCBDs on the polymer properties, a series of poly(ethylene-*co*-1-hexene) resins with very distinct, and in some cases bimodal crystalline distributions, were synthesized. The attractive feature of the resins in this study is that their molecular weight distributions are similar but each possesses a different SCBD, thus effectively minimizing the effect of molecular weight on the properties investigated.

It was found that the tensile properties of a copolymer could be controlled by the ratio of the crystalline species present in the sample. In this study, a balance of stiffness and toughness was exhibited by a copolymer containing a large proportion of crystalline material and a small fraction of material of lower crystallinity.

Keywords: Ethylene/α-olefin copolymers; Short chain branching distribution; Tensile properties

1. Introduction

Recently, there has been an emphasis on developing relations between microstructure and end-use physical/mechanical properties of polyolefins. With the advent of metallocene catalysts for olefin polymerization, there have been many claims on the ability to produce polymer with tailored microstructural distributions. Correspondingly, these distributions also result in resins with tailored physical/mechanical properties.

In a previous publication, we have reported a catalytic method that demonstrated the use of a heterogeneous metallocene catalyst to control the short chain branching distribution (SCBD) of ethylene/α-olefin copolymers [1]. By exploiting the multi-site behavior of these catalysts, it was possible to produce resins with broad and bimodal SCBDs but with similar and narrow molecular weight distributions. Ziegler–Natta LLDPE can also have a characteristically broad SCBD but the molecular weight distribution tends to be broader when compared to a metallocene-synthesized LLDPE [2]. Typically, for Ziegler–Natta resins, the comonomer content of the copolymer decreases as the molecular weight of the polymer chains increases.

Industrial methods to tailor the molecular weight distribution and SCBD of a polyolefin typically involve tandem or cascade reactors which produce the desired polymer depending on the polymerization conditions of each reactor [3]. Another method is to use combined catalyst systems, with each catalyst producing the desired polymer microstructural distribution [4]. Conventionally, tailored physical properties can also be achieved by the compounding and blending of polymers with the desired characteristics. Unfortunately, the blending of polymers is very energy intensive and it is inherently difficult to achieve uniform mixing.

It is well known that the underlying microstructure of polymers plays a critical role in determining their physical and mechanical properties. For linear polyolefins such as poly(ethylene/α-olefin) copolymers, both the molecular weight distribution and comonomer distribution of the polymer chains influence the crystallinity and density of the samples [5–9]. Above a critical molecular weight, it is sometimes found that the crystallinity will decrease with increasing molecular weight, due to the inability of the

* Corresponding author. Tel.: +1-519-888-4567 ext. 3436; fax: +1-519-888-6179.

E-mail address: jsoares@cape.uwaterloo.ca (J.B.P. Soares).

0032-3861/02/$ - see front matter
PII: S0032-3861(01)00666-8

longer chains to be incorporated in the crystalline structure [10–12]. More significantly, by increasing the number of short chain branches via incorporation of α-olefin comonomers such as 1-butene, 1-hexene, 1-octene, etc., the polymer's crystallinity and density can be reduced, since these side chains do not crystallize and are rejected into the amorphous or interfacial regions of the polymer [5,7]. The interplay between molecular weight and comonomer distribution influences the proportions of crystalline and amorphous polymer that determine its crystalline microstructure. The crystallinity and crystal structure are not only influenced by the microstructure of the polymer but also by the processing conditions that dictate the polymer's thermal history [8,11]. In terms of mechanical properties, a polymer's crystallinity influences its stiffness and toughness. In general, as the polymer crystallinity decreases, its flexibility increases. By lowering the density with the incorporation of comonomer to promote short chain branching, the polymer's ability to absorb and dissipate energy also increases [5,6].

In this study, we have produced a series of ethylene/1-hexene copolymers with tailored crystalline distributions while maintaining similar MWDs. By eliminating the effect of molecular weight, it is possible to investigate the net effect of crystalline distributions on the properties of these resins. This series of resins with controlled SCBDs was produced for comparing their tensile and dynamic mechanical properties.

2. Experimental

2.1. Sample production

Ethylene-1-hexene copolymer samples were produced with an in situ supported metallocene catalyst system [13]. This in situ system eliminates the need for a catalyst supporting stage by combining the catalyst preparation and polymerization in one-step. The resulting polymer has good particle morphology and high bulk density. These studies utilized *rac*-(ethylenebis(indenyl))zirconium dichloride (Strem Chemicals), a silica support with a high weight percent of methylaluminoxane (provided by Witco), and mixtures of trialkylaluminums such as trimethyl and triethyl aluminums. Slurry polymerizations with *n*-hexane as a solvent were carried out in a 1 l semi-batch autoclave reactor (Pressure Product Industries, LC Series) operating at 60°C and ethylene pressure of 150 psig. The initial concentration of 1-hexene in the reactor was 30 mol%. The polymerization runs were carried out under similar conditions and limited in such a way to minimize the drift in comonomer composition.

2.2. Microstructural characterization

The polymer samples were characterized for their molecular weight distributions using a Waters 150 CV high temperature gel permeation chromatograph (GPC) and a Viscotek 150 R viscometer. The mobile phase used was 1,2,4 trichlorobenzene operating at 140°C.

SCBDs were determined by crystallization analysis fractionation (CRYSTAF) in 1,2,4 trichlorobenzene using a CRYSTAF 200 unit (Polymer Char, Spain). The samples were dissolved at 160°C for 1 h and then cooled to 95°C to begin the analysis. The sampling temperatures ranged between 95 and 30°C at a cooling rate of 0.2°C/min. 1-Hexene comonomer compositions were determined by integrating the resulting CRYSTAF profiles while applying a calibration curve to relate the crystallization temperature and 1-hexene composition [14]. This calibration curve was previously determined by ^{13}C NMR.

Melting endotherms were determined using a TA 2100 differential scanning calorimeter (DSC). The samples were heated from 35 to 200°C at 10°C/min. To take into account the thermal history of the samples used for mechanical testing, the melting point and crystallinity were estimated from the first pass. The crystallinity was estimated by comparison of the DSC melting enthalpy to that of a perfect polyethylene crystal ($\Delta H \approx 289$ J/g) [9].

2.3. Mechanical testing

2.3.1. Tensile testing

Tensile properties were determined according to ASTM D638 using an Instron 4465 materials tester. Dog-bone shaped samples (type V) were melt-pressed at 200°C into a 3.175 cm mold plate and then air-cooled to room temperature. The samples were tested at a displacement rate of 25 mm/min and the grip-to-grip length was 3 cm. The sample yield and ultimate break strengths were determined from the force versus displacement curves during deformation of the sample. After testing, the increase in the gage length as compared to the original was used to determine the overall % elongation.

2.3.2. Dynamic mechanical analysis

Dynamic mechanical properties were measured by a Rheometrics DMTA V mechanical spectrometer. These samples were also melt pressed into rectangular bars (20 mm × 10 mm × 3 mm) under the same conditions as reported above. Storage and loss moduli were measured in single cantilever mode over a temperature range −150 to 100°C at a scanning rate of 2°C/min, a frequency of 1 Hz and a strain of 0.05%. Frequency sweeps were performed over the range 0.1–100 Hz at room temperature and 0.05% strain.

3. Results and discussion

As discussed previously, it was found that with certain in situ supported metallocene catalyst systems it is possible to control the SCBD of ethylene copolymers by simply varying the amount and type of alkylaluminum activator

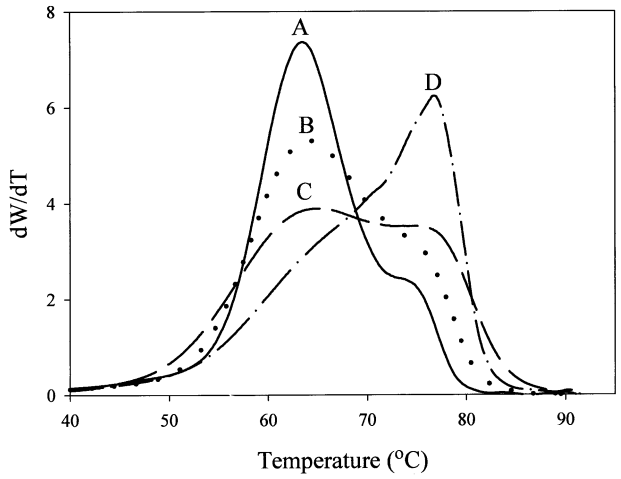

Fig. 1. Comparison of CRYSTAF profiles of tailored ethylene/1-hexene copolymers.

present in the polymerization recipe [1]. Based on the nature of the individual activators under copolymerization conditions, trimethylaluminum (TMA) produces a copolymer with unimodal SCBDs, whereas triethyl (TEA) or triisobutyl aluminium (TIBA) activators produce copolymers with broad and bimodal SCBDs; upon mixing any two types of activators, a blended distribution results.

For this study, the samples were prepared under similar polymerization conditions and only differed by the amount and type of each activator used. The four resins were prepared by varying the mixing ratio of TMA and TEA. Sample A was prepared with 100% TMA, sample B with 50% TMA and 50% TEA, sample C with 25% TMA and 75% TEA and sample D with 100% TEA.

The CRYSTAF profiles of the polymers made with these mixed activator systems are shown in Fig. 1. A CRYSTAF profile can be correlated with the SCBD of a polymer. With the use of a temperature-composition calibration curve as shown in Fig. 2, it is possible to relate the polymer's crystallization temperature with its % incorporated comonomer or

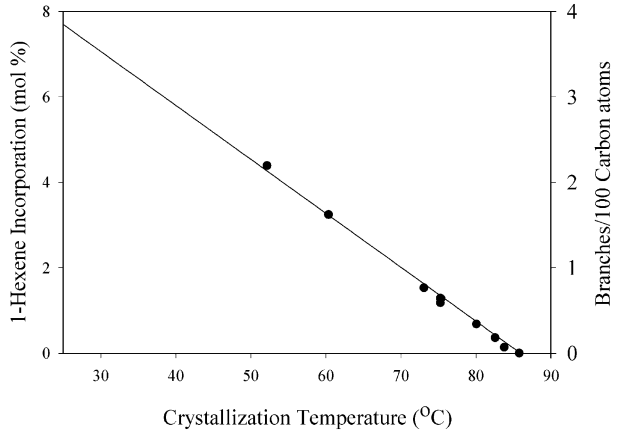

Fig. 2. Calibration curve relating the CRYSTAF crystallization temperature and 1-hexene incorporation in the copolymer.

branching frequency (as determined from ^{13}C NMR). It is clearly shown that samples A through D have very distinct and bimodal crystallinity distributions. Two distinct regions are present, a homopolymer-like region present at higher crystallization temperatures between 70 and 80°C, and a copolymer-like region, present at lower temperatures between 50 and 70°C. It should be noted that the proportion of homopolymer increases from sample A to D. A comparison of the corresponding molecular weight distributions is shown in Fig. 3. The MWDs of the four resins are quite similar. The number average molecular weights of these samples, listed in Table 1, are in the range of 40,000 g/mol. However their polydispersity indices do vary due to tailing in the high molecular weight region. This tailing is probably due to drift in comonomer concentration during the polymerization. As the polymerization proceeds to high yields, the comonomer concentration decreases and higher molecular weight material is formed. Nonetheless, the presence of this tail cannot account for the large differences in the SCBDs observed for these samples. In a previous study, we have demonstrated that ethylene copolymers similar to the ones studied here, have SCBDs with uniform and narrow molecular weight distributions [1]. Overall, these molecular weight distributions are similar in shape for the comparison of the SCBDs shown in Fig. 1. Also shown in Table 1 are the estimates of the overall 1-hexene comonomer content as determined from the temperature-composition calibration curve. As shown, the comonomer content decreases from samples A to D. Sample A contains an estimated average of 4.0 mol% of 1-hexene, while sample D contains 2.8 mol%, which also translates, in terms of backbone atoms, to a range from 2.0 to 1.4 branches per 100 carbons. It is assumed that with this level of branching, the copolymer/homopolymer phases are miscible. Rana et al. have reported that LLDPEs with up to four branches per 100 carbons were miscible with polyethylene homopolymer [15]. Consequently, one can assume that copolymers with blended crystalline distributions are also miscible. Also shown in Table 1 are the estimates of the % crystallinity from DSC of the samples

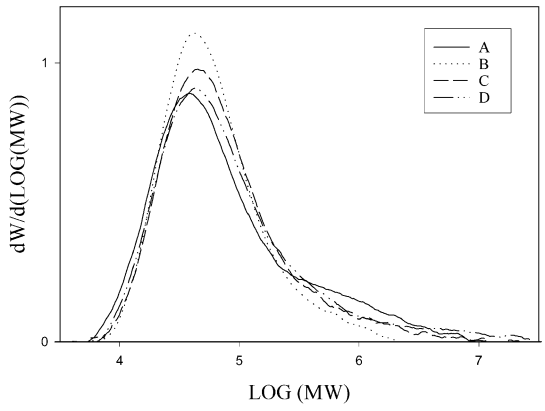

Fig. 3. Comparison of MWDs of tailored ethylene/1-hexene copolymers.

Table 1
Microstructural properties of ethylene/1-hexene resins

Sample[a]	$\bar{M}_n$[b] (g/mol)	$\bar{M}_w/\bar{M}_n$[b]	1-Hexene content[c] (mol%)	Average branching frequency[c] (branches per 100 C)	Melting peak[d] (°C)	Crystallinity[e] (%)
A	39,700	6.7	4.0	2.0	114.6	43.3
B	41,400	2.5	3.6	1.8	117.8	45.2
C	43,800	4.9	3.4	1.7	119.8	45.6
D	43,800	6.3	2.8	1.4	122.3	53.2

[a] Polymerization conditions: $[Et(Ind)_2ZrCl_2] = 13.3$ mmol/l, Al/Zr = 500, ethylene pressure = 150 psig, [1-hexene] = 30 mol% feed (41 ml), polymerization temperature = 60°C, stirring rate = 400 rpm.
[b] As determined from GPC analysis based on a universal calibration curve derived from narrow polystyrene standards.
[c] As determined from an integrated CRYSTAF profile and 1-hexene temperature-composition calibration curve.
[d] As determined by DSC. Note that these samples exhibited very broad melting distributions.
[e] Crystallinity estimates based on DSC melting enthalpy as compared to a perfect crystalline polyethylene ($\Delta H \approx 289$ J/g)[9].

air-cooled from melt to room temperature. The corresponding melting profiles are shown in Fig. 4. As seen, these melting profiles correspond well to the SCBDs measured by CRYSTAF. For samples B and C, the DSC melting profiles indicate the presence of two distinct populations of crystalline species.

A representative comparison of the force versus displacement curves during the deformation of the four resins is shown in Fig. 5. In general, it was observed that all of the samples exhibited localized yielding and cold drawing that is characteristic to semi-crystalline polymers. Qualitatively examining the yielding region, it was observed that a narrowing of the yield zone occurred from sample A to D. For samples A and B, a broad yielding region was observed, which could be classified as a double yield point. This double yield behavior has also been observed by others for polyethylene copolymers [6–8,16]. This phenomenon may be caused by a partial melt-recrystallization process. At the first yield point, temporary plastic deformation occurs, followed by a recoverable recrystallization of the lamellae. The second point is the onset of permanent plastic deformation in which the lamellae are destroyed [16]. Grahm et al. have reported that this type of behavior may be related to the degree of crystallinity and thermal history

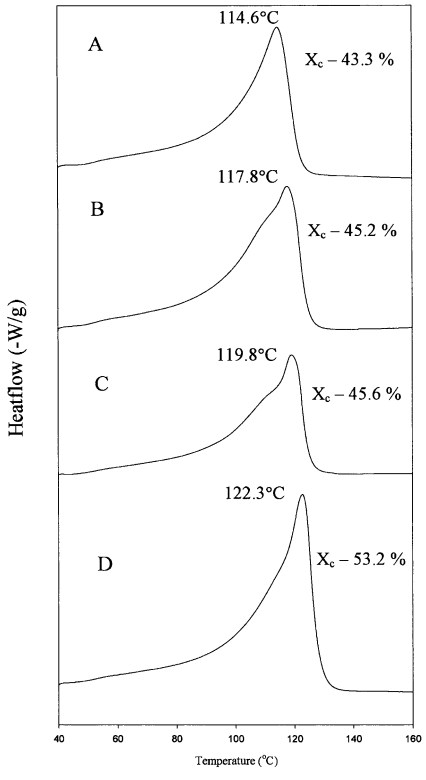

Fig. 4. DSC melting profiles of tailored ethylene/1-hexene copolymers.

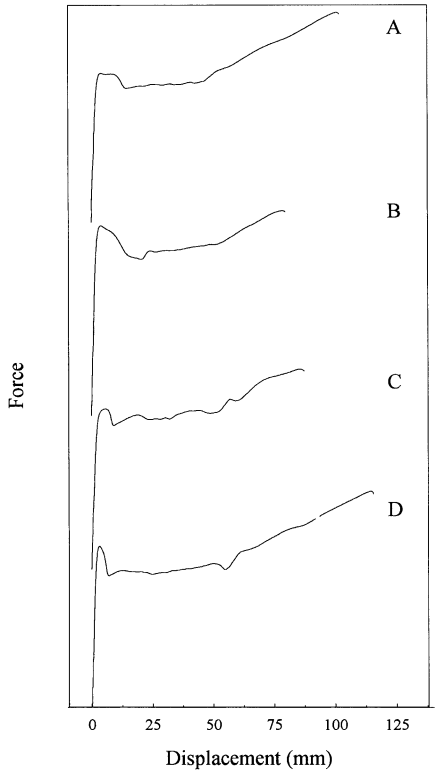

Fig. 5. Tensile deformation comparison of tailored ethylene/1-hexene resins.

of the polymer which both can influence the structure and morphology of the crystallites [8]. Bensason et al. reported that with a decrease in density, the yield maximum broadens up to a point where it then becomes indistinguishable and no yield maximum is observed [6]. Similarly for these samples, it appears that the yielding region broadens with a decrease in crystallinity or increase in comonomer content. Given the bimodal nature of the SCBDs in these samples, it seems that increasing the proportion of higher crystalline material results in a narrower yield maximum.

A summary of the measured tensile properties is shown in Table 2. The tensile strength at yield increases while increasing the proportion of higher crystalline material. This increase in tensile strength is closely related to the stiffness of the samples. Estimates of the sample's overall crystallinity from DSC show that crystallinity increases from samples A to D (see Table 1), which confirms the increase in stiffness. The tensile strengths at yield of samples B and C predictably fall within the ranges of A and D. After the material exceeds the yield point and deforms, the ultimate tensile strengths (at break) also show that sample D has the highest value and sample A the lowest. In regards to the % elongation, which can be a measure of the material's ability to deform and dissipate energy, it was found that sample D had the highest value at 440%. It was expected that the sample with the highest comonomer content, such as sample A, would exhibit the highest % elongation at break. A sample with low crystallinity possesses a large fraction of amorphous polymer. It is the slippage and disentanglement of amorphous polymer that allows it to deform. In the literature, Jordens et al. noticed that with decreasing crystalline density, a higher % elongation was observed [11]. Bensason et al. also observed for low crystalline poly(ethylene-*co*-1-octene) copolymers that, with increasing comonomer content, an increase in strain % was observed [6,17]. The % elongation of sample A was quite high at 373% but sample D was even higher. Although the crystallinity of sample D was the greatest of the four samples studied, it exhibited the highest stiffness and ductility. Both sample B and C demonstrated intermediate values of tensile strengths and showed lower % elongations. Generally, for copolymers with unimodal SCBDs, the crystallinity of the polymer relates well to the stiffness and % elongation [5–7,17]. At low strain, the sample's crystallinity is the dominant factor during a deformation process but at high strains the role of entanglements prevails [17,18]. From the examination of the SCBDs for these resins (Fig. 1), it can be seen that sample D has a tail in the lower crystalline region. It is believed that this balance of low and high crystalline material resulted in a blending of the tensile properties. This balance of properties may be explained by the presence of this comonomer tail. This less crystallisable polymer would increase the number of entanglements and increase the amount of tie material. Generally, tie molecules are considered as chains that bridge the amorphous and crystalline regions. The presence and amount of tie molecules have been known to influence the mechanism of failure [19]. A transition from a ductile to brittle failure mechanism sometimes occurs if too few tie molecules or entanglements are present. These tie molecules can also affect the strain hardening behavior [11]. As a sample's crystallinity decreases (via branching or thermal treatment) or with an increase in molecular weight, the number of tie molecules present in the amorphous regions increases [5,19,20]. The most effective tie molecules have been shown to be high in molecular weight and high in comonomer content up to a limiting value. From the results above, sample D was the toughest by displaying the highest percent elongation and tensile stress at break. Sample D was followed by sample A. It is believed that sample A performed well due to its lower crystallinity. To account for the toughness of the polymers observed in this study, two hypotheses will be given. For these samples, the molecular weight distributions as shown in Fig. 3 showed slight tailing in the high end of the distribution. This is also reflected in both samples possessing the largest PDIs at 6.3 for sample D and 6.7 for sample A. As mentioned previously, it is believed that these tails are lower in comonomer content due to the slight drift in comonomer concentration during the polymerization. It is possible that this small amount of high molecular weight material increased the number of entanglements and resulted in the increase in toughness that was observed. Under this assumption, it would be reasonable to assume that sample A would show the largest % elongation since it has the broadest MWD and highest comonomer content. However, sample D exhibited the highest % elongation. It is believed that the presence of the low crystalline tail shown in the SCBD increased the number of entanglements and increased the amount of tie material. The superior toughness of sample D is probably due to a combination of sample D's high crystallinity and large comonomer tail.

As a comparison to the tensile properties measured above, the solid-state dynamic mechanical responses of these resins were measured. Within the temperature range studied, it can be seen that the samples exhibited the characteristic γ-, β- and α-transitions, as indicated by the changes in tan delta shown in Fig. 6. Although there is much

Table 2
Tensile property data of ethylene/1-hexene copolymers (Testing conditions: ASTM D638 (type V), 3.175 mm thickness, displacement rate 25 mm/min, grip to grip length 3 cm)

Sample	Tensile strength at yield (kPa) (±666)[a]	Tensile strength at break (kPa) (±1178)[a]	Elongation at break (%) (±43)[a]
A	11,490	15,600	373
B	12,110	14,780	315
C	13,800	14,880	330
D	14,150	19,500	440

[a] Calculated standard deviations based on replicate testing.

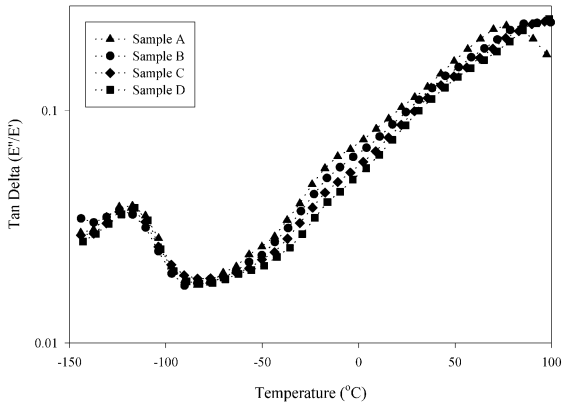

Fig. 6. Tan delta comparison of tailored ethylene/1-hexene copolymers carried out at 1 Hz.

debate on the existence and nature of these transitions, it is believed that they are linked to the motions of the amorphous and crystalline portions of the polyethylene chains [6,21–23]. Examining the tan delta behavior (Fig. 6), the γ-transition that is often associated with the glass transition temperature of the amorphous polymer was observed around −120°C. The β-transition that is sometimes linked to motion of the branched segments of the chain occurred between −25 and 0°C. This β-transition can also be related to the comonomer content of the polymer [6,22]. As shown, sample A exhibited the largest tan delta during this transition followed by samples B, C and D, in the order of decreasing comonomer content. The α-transition was observed above 50°C and this may be linked to the gradual motion of main chain units within the crystallites before the onset of melting.

The sample's ability to dampen energy at room temperature is reflected by the tan delta that decreases with the increase in crystallinity of the copolymers (as in Fig. 6). Comparing the elastic response of all the samples, it is shown in Fig. 7 that the storage moduli decreased with an increase in temperature. For these polymer samples, their

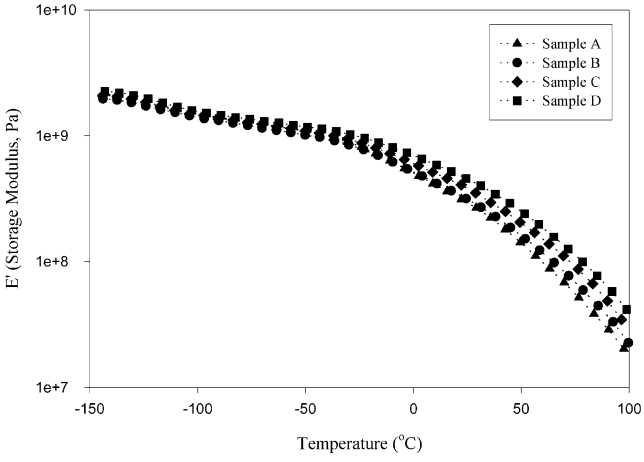

Fig. 7. Elastic response comparison of tailored ethylene/1-hexene copolymers carried out at 1 Hz.

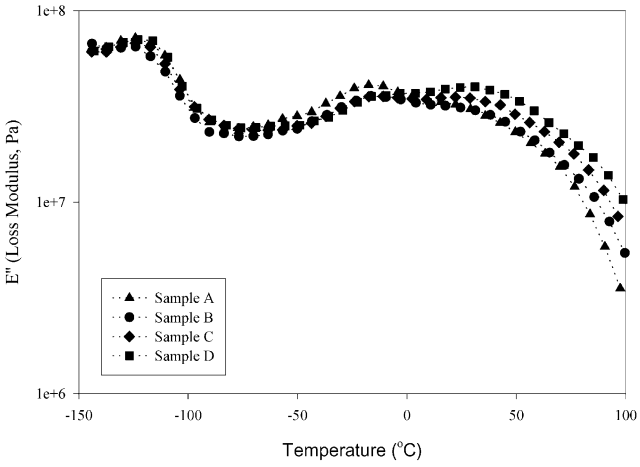

Fig. 8. Loss response comparison of tailored ethylene/1-hexene copolymers carried out at 1 Hz.

elasticity decreased as the samples softened with the increase in temperature. At room temperature, the storage moduli of resins A through D increased. The increase in stiffness of the samples is a reflection of the increase in the sample's crystallinity that was also observed in the comparison of the tensile strengths (Table 2). Comparing the loss responses of the samples in Fig. 8, it can be seen that at different temperatures the samples passed through γ-, β- and α-transitions. The loss modulus can be associated with the energy lost due to friction and internal chain motion [23]. It is believed that this energy loss is related to the relaxation of the entanglements present in the microstructure. The relaxation of these entanglements at a given frequency may give an indication to the high strain deformation behavior in the tensile study. At room temperature it is shown that the loss modulus decreases from sample D to A (Fig. 8). This trend is different from the one observed in the tensile study in which sample A and sample D exhibited the greatest % elongation at break. Although the trend reported from the loss modulus is different, it is noted that the loss moduli sequence of the samples changed with temperature. At around 0°C a crossover of the E'' modulus occurs, changing the order to sample D, A, C and B. At this temperature, the order of the E'' moduli for these samples is closer to the one observed in the tensile study for the % elongation at break. It is well known that these dynamic responses from oscillatory measurements are frequency and temperature dependent [23]. As the frequency of the test increases, the polymer chains have less time to relax and can appear to be stiffer. At lower temperatures, the relaxation of the polymer chains is slowed which also results in an increase in stiffness. For these oscillatory measurements, the analysis was carried out at 1 Hz. The tensile test was carried out at a higher strain rate than 1 Hz. Thus the process of a tensile test would presumably be better represented at a higher frequency since the strain rate used in these experiments was fairly high.

Fig. 9 shows the frequency dependence of the samples at

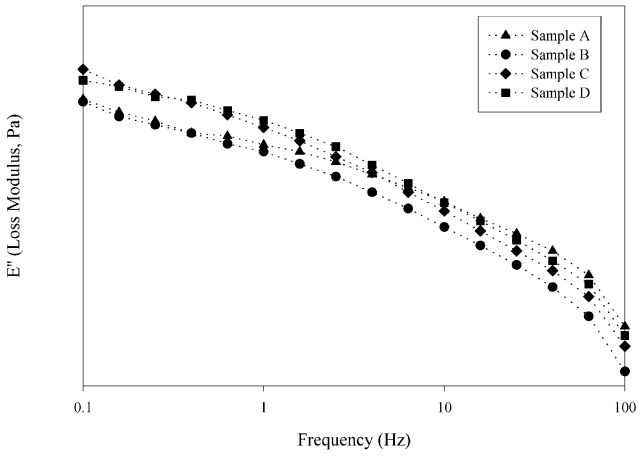

Fig. 9. Frequency dependence of E'' (loss modulus) of tailored ethylene/1-hexene copolymers at room temperature.

room temperature. As shown, the loss response of the samples changed with frequency. Sample A exhibited an increase in its loss response with an increase in frequency. At approximately 10 Hz, a crossover of the E'' of sample A and sample D occurred. At this frequency the samples loss response compares well to the % elongation at break of the tensile test data (Table 2). Despite the consistency of the results, it is not clear on the relation between the high strain deformation behavior as in the tensile test and low strain behavior by DMTA. It is possible that the loss moduli obtained from the linear viscoelastic region is sensitive to a portion of the microstructure such as the relaxation of the entanglements that contributes to the high strain properties.

Overall, both tensile and dynamic mechanical properties have shown that sample D exhibited the greatest toughness. This sample had a bimodal SCBD with a large portion of high crystalline and a smaller fraction of lower crystalline material. As a result, this sample displayed a balance of stiffness and toughness. This balance of properties can be explained by the distribution of crystalline material as measured by CRYSTAF (Fig. 1).

4. Conclusions

It has been demonstrated how the microstructure and properties of metallocene-synthesized polymers can affect their mechanical properties. Using a heterogeneous metallocene catalyst system with mixtures of alkylaluminum activators, it was possible to control the crystalline distribution of polyethylene copolymers. Using this method, a series of poly(ethylene-*co*-1-hexene) resins with very distinct crystalline distributions but with similar molecular weight distributions was produced.

Given the unique characteristics of these resins, i.e. resins with broad/bimodal crystalline distributions but having uniform molecular weight distributions, structure-property studies have shown that the mechanical properties of these resins can be modified. Tensile testing and dynamic mechanical analysis demonstrated how an ethylene copolymer with portions of highly crystalline and low crystalline material exhibits a balance of stiffness and toughness, thus demonstrating how the structure and properties of an ethylene copolymer can be tailor-made with a metallocene catalyst system.

Acknowledgements

The authors would like to thank the Natural Sciences and Engineering Research Council of Canada (NSERC) for financial support.

References

[1] Li Pi Shan C, Chu KJ, Soares JBP, Penlidis A. Macromol Chem Phys 2000;201:2195–202.
[2] Garbassi F, Gila L, Proto A. Polym News 1994;19:367–71.
[3] Scheirs J, Bohm L, Bout L, Leevers PS. Trends Polym Sci 1996;4:408–15.
[4] Soares JBP, Kim JD, Rempel GL. Ind Engng Chem. Res. 1997;36:1144–50.
[5] Kale L, Plumley T, Patel R, Redwine O, Jain P. J Plast Film Sheeting 1995;12:27–40.
[6] Bensason S, Minick J, Moet A, Chum S, Hiltner A, Baer E. J Polym Sci Part B: Polym Phys 1996;34:1301–15.
[7] Simanke AG, Galland GB, Neto RB, Quijada R, Mauler RS. J Appl Polym Sci 1999;74:1194–200.
[8] Grahm JT, Alamo RG, Mandelkern L. J Polym Sci Part B: Polym Phys 1997;35:213–23.
[9] Xu X, Xu J, Feng K, Chen W. J Appl Polym Sci 2000;77:1709–15.
[10] Hosoda S, Uemura A. Polym J 1992;24:939–49.
[11] Jordens K, Wilkes GL, Janzen J, Rohlfing DC, Welch MB. Polymer 2000;41:7175–92.
[12] Nunes RW, Martin JR, Johnson JF. Polym Engng Sci 1982;22:205–28.
[13] Chu KJ, Soares JBP, Penlidis A. J Polym Sci Part A: Polym Chem 2000;38:462–8.
[14] Monrabal B. J Appl Polym Sci 1994;52:491–505.
[15] Rana D, Lee CH, Cho K, Lee BH, Choe S. J Appl Polym Sci 1998;69:2441–50.
[16] Brooks NWJ, Duckett RA, Ward IM. Polymer 1999;40:7367–72.
[17] Bensason S, Stepanov EV, Chum S, Hiltner A, Baer E. Macromolecules 1997;30:2436–44.
[18] Doyle MJ. Polym Engng Sci 2000;40:330–5.
[19] Lustiger A, Markham RL. Polymer 1983;24:1647–54.
[20] Channel AD, Clutton EQ. Polymer 1992;33:4108–12.
[21] Nitta KH, Tanaka A. Polymer 2001;42:1219–26.
[22] Simanke AG, Galland GB, Freitas L, da Jornada JAH, Quijada R, Mauler RS. Polymer 1999;40:5489–95.
[23] Menard KP. Dynamic mechanical analysis – a practical introduction. New York: CRC Press, 1999.